J Appl Electrochem (2010) 40:777–782
DOI 10.1007/s10800-009-0056-3

ORIGINAL PAPER

Influence of cobalt on manganese incorporation in Ni–Co coatings

Meenu Srivastava · V. K. William Grips · K. S. Rajam

Received: 3 September 2009 / Accepted: 4 December 2009 / Published online: 19 December 2009

Abstract The effect of alloying <1 wt% Mn with plain Ni, Ni–Co alloys and plain Co coatings in terms of the structure and properties has been studied. The alloys were electrodeposited from an additive free sulphamate electrolyte. The Mn concentration in the electrolyte was maintained at 5 g L^{-1} so as to obtain <1 wt% Mn content in the alloy coatings. The Energy Dispersive X-ray analysis (EDX) showed that the Mn content reduced from 0.97 to 0.05 wt% with increase in Co content from 0 to 98 wt% in the alloy coating. An increase in microhardness was obtained on the addition of Mn to Ni/Ni–Co alloys. The X-ray diffraction (XRD) and Scanning Electron Microscopy (SEM) studies revealed a change in crystal structure and morphology. Pin-on-disc tribology test revealed better wear performance of Ni–18 wt%Co–Mn alloy coating compared to the other Ni–Mn/Ni–Co–Mn alloy coatings.

Keywords Ni–Co–Mn alloy · Ni–Co alloy · Microstructure · Mechanical properties

1 Introduction

Hard nickel coatings can be deposited from various electrolytes in the presence of sulphur containing organic additives. These deposits display good mechanical properties, but their use at temperatures greater than 400 °C is restricted, owing to sulphur embrittlement, which leads to lower strength [1, 2]. This embrittlement can be overcome by co-depositing Mn along with Ni, as Mn tends to form MnS with sulphur. The MnS gets deposited as scattered globules along the inter-grain boundaries [3]. Also, MnS imparts enhanced thermal stability due to its resistance to both anneal softening and grain growth [4]. In addition, the tensile strength of Ni–Mn deposits are 3–4 times higher than wrought Ni and hence are used as mechanical microsystem components [1, 5–10]. In recent times, these alloys are gaining importance as corrosion resistant coatings for mild steel. However, co-depositing Mn with Ni is very difficult because of the high reduction potential of Mn^{2+} −1.18 V, whereas for Ni^{2+} it is −0.25 V. Some investigators have been successful in depositing small amounts of Mn (<1 wt%) [7].

An alternate method of enhancing the mechanical properties of Ni is by alloying it with Co [11–14]. Ni–Co particulate composites have been studied and have been reported to display improved mechanical properties [11, 13, 15]. Co enhances the ductility at moderate temperatures without affecting the tensile strength. Thus to obtain an alloy, which exhibits superior mechanical properties over wide temperature range and also improved corrosion resistance, Ni–Co–Mn alloy can be a suitable material. This objective has led to the present investigation. The problem likely to be encountered is the deposition of Mn in the presence of Co. Theoretically, Mn does not deposit with most metals, but it does to some extent with iron group metals [16]. To the knowledge of the investigators, the influence of <1 wt% Mn on the structure and wear of Ni–Co alloy coatings has not been reported. A low Mn content has been chosen as an increase resulted in a stressed deposit [9]. In the present study, the effect of <1 wt% Mn addition to Ni–Co alloys containing different Co contents has been studied in terms of the structure, microhardness and wear performance.

M. Srivastava (✉) · V. K. William Grips · K. S. Rajam
Surface Engineering Division, National Aerospace Laboratories (CSIR), Post Bag No. 1779, Bangalore 560 017, India
e-mail: meenu_srivas@yahoo.co.uk

2 Materials and methods

The electrodeposition was carried out employing an additive free sulphamate electrolyte comprising of nickel sulphamate 275 g L^{-1}, nickel chloride 6 g L^{-1} and boric acid 30 g L^{-1}. Suitable amount of cobalt sulphamate was added to the electrolyte so as to obtain 1–50 g L^{-1} of Co as metal. The Mn content was maintained as 5 g L^{-1} (as $MnCl_2$) and anti-pitting agent (Sodium Lauryl Sulphate) 0.2 g L^{-1}. The deposition was carried out for 8 h at pH 4.0, under ambient conditions, employing a current density of 0.8 A dm^{-2} so as to obtain a coating of average thickness 55 ± 3 μm. The pH was electrometrically followed and maintained using sulphamic acid. A current efficiency of around 85 ± 2% was observed for all the coatings. A comparison has been made with Ni and Ni–Co alloy coatings obtained under the abovementioned conditions and discussed in detail elsewhere [12]. The sample preparation of the coating for metallographic studies is described in detail elsewhere [12]. The Mn and Co content in the coatings were determined using EDX, which is affiliated with the SEM, Leo 440I. The topographical information of the coatings was obtained by employing the SEM and Atomic Force Microscope (AFM). The crystal orientation was determined using Rigaku X-ray Diffractometer (XRD) employing Cu K_α radiation of wavelength 0.154 nm. The crystallite size was calculated using the Scherrer equation [17] with reference to the (200) reflection for alloys with fcc phase structure and (100) for those possessing hcp structure. The microhardness was determined using a microhardness tester Micromet 2103, by indenting across the cross-section of the coatings. The values reported are the average of five measurements made at different locations. Pin-on-disc wear testing (DUCOM, India) was adopted to understand the wear performance of various Ni–Co–Mn alloy coatings at ambient temperature and under dry sliding conditions. The coating was deposited on a brass hemispherical pin of diameter 12 mm and tested against an EN31 hardened steel disc. The experimental conditions adopted for wear testing were load 9.8 N, track radius 30 mm, disc speed 200 rpm, humidity 45% and sliding speed of 0.628 m s^{-1}. The wear track profile of the worn pin and disc was observed using optical microscope at 50×. The nature of wear products was identified from the Raman spectrum of the wear track on the worn discs of few representative Ni–Co–Mn alloy coatings.

The Raman spectra on the disc of various Ni–Co–Mn coating wear tracks were recorded with a DILOR-JOBIN-YVON-SPEX (Paris, France) integrated Raman Spectrometer (Model Labram). The spectrometer uses a microscope coupled confocally to a 300 mm focal length spectrograph equipped with two switchable gratings (300 and 1,800 grooves mm^{-1}). A He–Ne 20 mW laser beam was used as the excitation source. The laser was totally reflected by a notch filter toward the sample under a microscope, and the Raman scattering was totally transmitted through the notch filter towards the confocal hole and entrance slit of the spectrometer. The spectrum was recorded in a Peltier cooled charge coupled device CCD detector. The data was collected with a 10-s data point acquisition time in the spectral range of 100–1,200 cm^{-1} and 1,000-1,900 cm^{-1}.

3 Results and discussion

3.1 Manganese incorporation

The effect of Co content on the Mn incorporation is shown in Fig. 1. It is seen that the maximum content of Mn incorporated in Ni/Ni–Co alloy matrix is 0.97 wt%, present in Ni–Mn coating. The probable mechanism involved in the incorporation of Mn is that as the deposition efficiency is 85 ± 2% the remaining energy is spent on hydrogen evolution. The atomic hydrogen evolved on the cathode being a strong reducing agent reduces the manganese ion leading to its inclusion in the deposit [7]. Ni–Co alloys with Co contents of 18, 47 and 87 wt% showed a reduction in Mn incorporation from 0.4 to 0.05 wt% although the Mn content in the electrolyte was maintained a constant (Fig. 1). No change in Mn incorporation (0.05 wt%) is observed in a plain Co matrix. This shows that Mn deposition becomes difficult in going from a Ni base to a Co base matrix. This can be associated to the fact that Ni holds hydrogen evolved during electrodeposition loosely, thus making it available to catalyze the manganese reduction leading to higher incorporation in a Ni and Ni rich Ni–Co alloys compared to Co rich alloys [16].

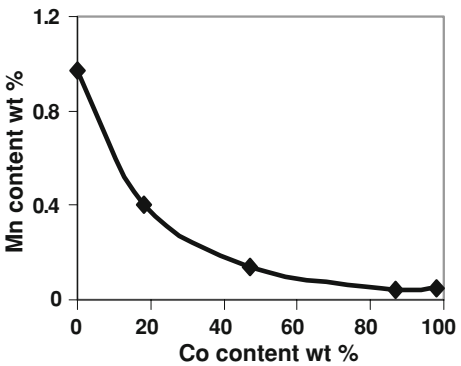

Fig. 1 Effect of Co content on Mn incorporation in Ni/Ni–Co alloy coatings

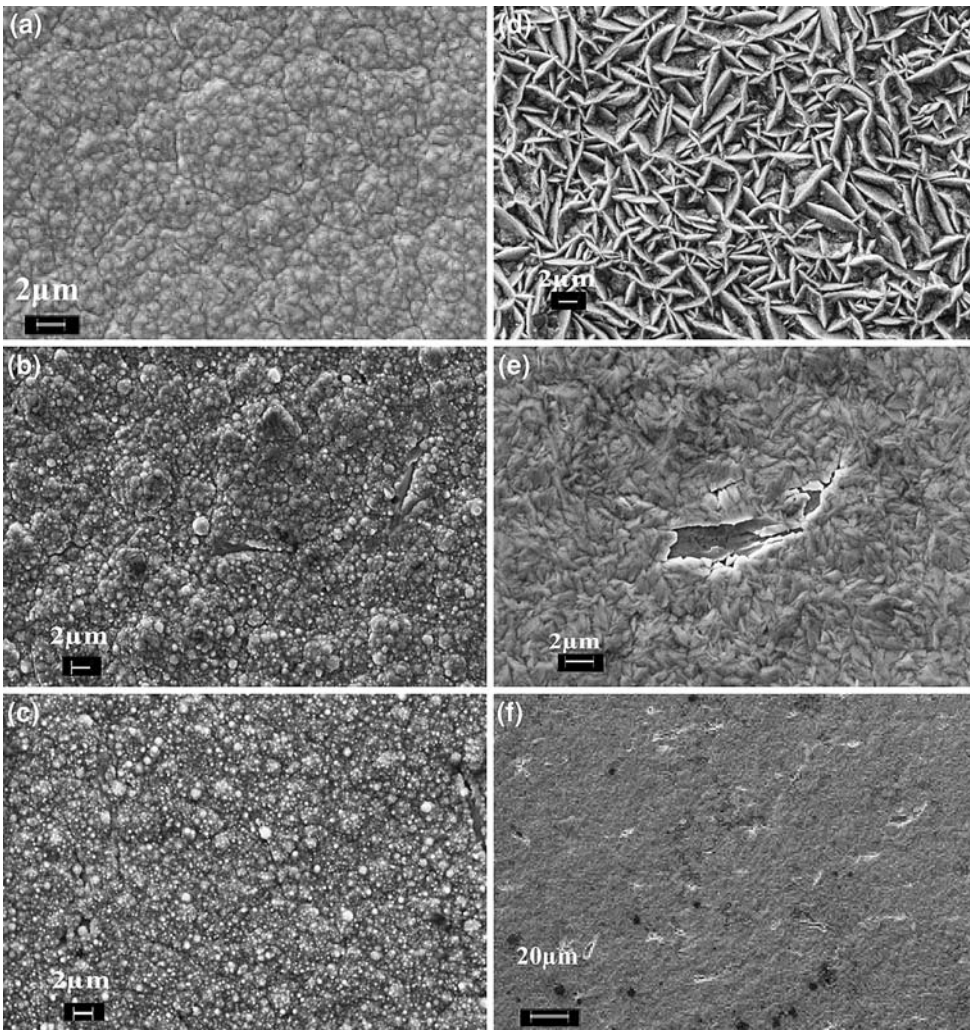

Fig. 2 Surface morphology at 2,500× of **a** Ni–Mn, **b** Ni–18Co–Mn, **c** Ni–47Co–Mn, **d** Ni–87Co–Mn, **e** Co–Mn coating and **f** Co–Mn coating at 500× showing fine cracks distributed throughout the surface

3.2 Morphology

Surface morphologies of Ni/Ni–Co–Mn alloys deposited from a sulphamate electrolyte are depicted in Fig. 2. The morphology of Ni changed from coarse polyhedral crystals to smaller crystallites in the presence of 0.97 wt% Mn (Fig. 2a, [12]). The alloying of Ni–18Co with 0.40 wt% Mn resulted in a change in morphology from polyhedral (Ni–18Co alloy) to nodular crystallites (Fig. 2b, [12]). A fine nodular morphology is observed for Ni–47Co alloy with 0.14 wt% Mn (Fig. 2c) and a change from nodular to ridged morphology is observed for Ni–87Co–0.04Mn alloy (Fig. 2d). This change in morphology is due to the variation in Co content in the matrix. A similar change has been observed by the authors for Ni–Co alloys [12]. Although the presence of Mn in Co matrix is insignificant, a diffusely ridged morphology with small cracks distributed throughout the Co matrix is observed on the surface of Co–Mn coating (Fig. 2e). The cracks could be due to the greater lattice mismatch between Co (hcp) and Mn (bcc), resulting in stress induced cracks (Fig. 2f, [18]). Figure 3a, b are the surface topographies of Ni–0.97 wt% Mn and Co–0.04 wt% Mn coatings. It is seen that the surface roughness of Ni–Mn coating is 358 nm while that of Co–Mn coating is 300 nm.

3.3 Structural characterization

The XRD diffractogram of the various coatings is shown in Fig. 4. The coatings are polycrystalline in nature and there are no reflections corresponding to Mn as the content is <1 wt%. The Ni–Mn coating exhibited a preferred and predominant (200) reflection which is similar to that exhibited by plain Ni coating [12]. The Ni–18Co–Mn alloy exhibited a random orientation with (111) predominant reflection. (220), (200) and (311) reflections are also observed. A change in the predominant orientation from (200) to (111) is observed between the Ni–18Co, Ni–18Co–Mn alloy and Ni–Mn, Ni–18Co–Mn alloy coatings [12]. This may be the cause for the difference in surface

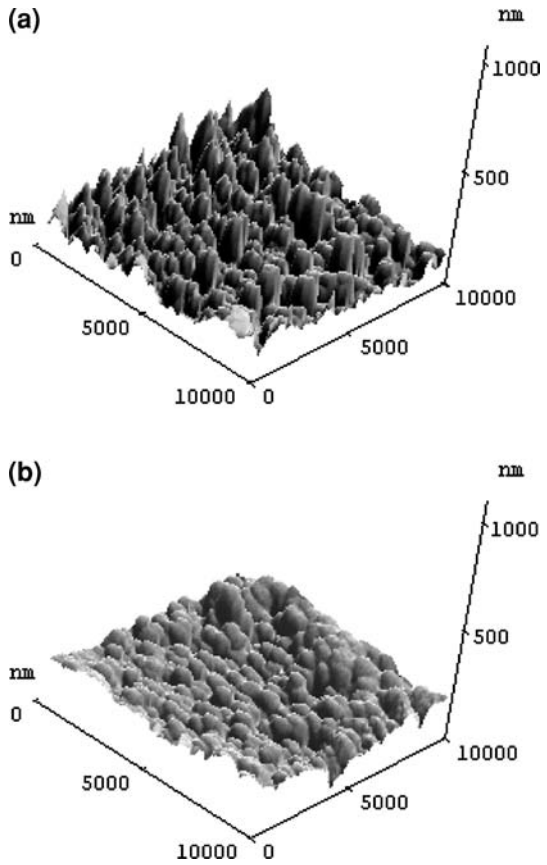

Fig. 3 Surface topography of **a** Ni–Mn and **b** Co–Mn coatings using AFM

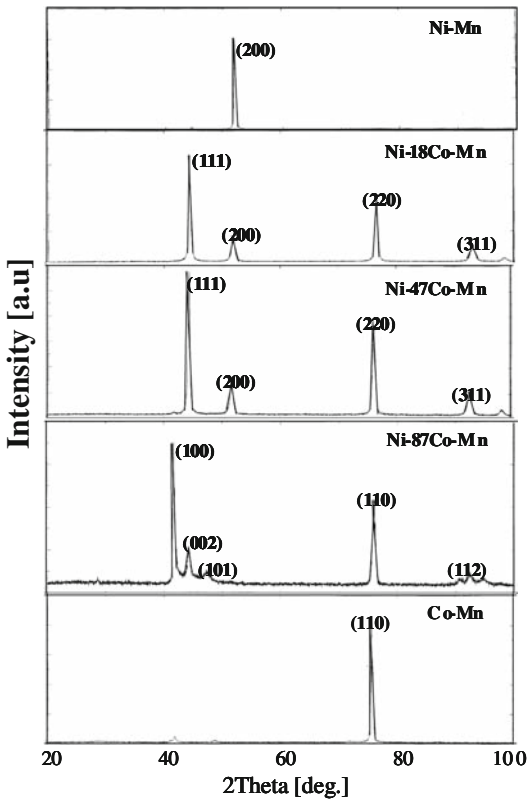

Fig. 4 XRD diffractogram of Ni–Mn, Ni–18Co–Mn, Ni–47Co–Mn, Ni–87Co–Mn and Co–Mn alloy coatings

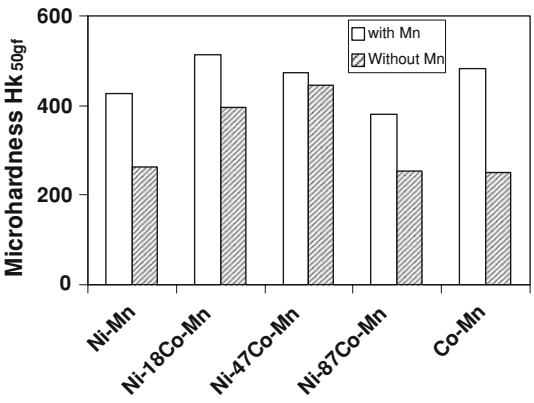

Fig. 5 Comparative microhardness of Ni/Ni–Co and Ni–Mn/Ni–Co–Mn alloy coatings

morphology among the two alloy pairs. The diffraction pattern of Ni–47Co–Mn alloy coating is similar to that of Ni–18Co–Mn alloy. The crystal structure is observed to be fcc for all the Ni rich coatings. The crystallite size was determined (based on (200) reflection) to be 23 nm for Ni–Mn coating and it reduced to 12 nm for Ni–18Co–Mn coating. However, no such reduction was observed between plain Ni and Ni–18Co alloy coatings [12]. The reduction in crystallite size in the presence of Mn can be related to the difference in the predominant orientations. A similar correlation between Mn content, grain size and texture has been reported by Yang et al. [8]. Further, as no change in the diffraction pattern is observed for Ni–47Co–0.14Mn coating no variation in the crystallite size is seen between Ni–18Co–0.4Mn and Ni–47Co–0.14Mn coatings. Although, a reduction in size was observed for Ni–18Co and Ni–47Co alloy coatings [12].This is due to the fact that the influence of Mn on crystallite size diminishes with a decrease in its content [8]. Ni–87Co–Mn coating exhibited an hcp crystal structure with a random orientation and a predominant (100) reflection. (110), (002), (101) and (112) reflections are also visible (Fig. 4). A change in the preferred orientation of the crystallites is seen between the Ni–87Co alloy (110) and Ni–87Co–Mn alloy (100) coatings [12]. Similarly, hcp Co–Mn coating exhibited a preferred and predominant (110) reflection, which is different from that of the plain Co coating (100) [12]. The crystallite size determined with reference to (110) reflection was 15 and 28 nm for Ni–87Co–Mn and Co–Mn coatings, respectively. A change in the crystal structure from fcc to hcp is seen between Ni–47Co–Mn and Ni–87Co–Mn coatings. This is due to the increase in the Co content in the matrix from 47 to 87 wt%, which is also responsible for the marginal increase in the crystallite size from 12 to 15 nm.

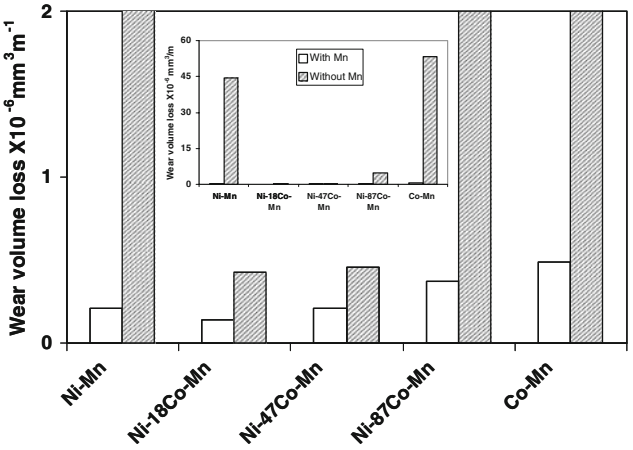

Fig. 6 Comparison at low wear volume loss between Ni/Ni–Co and Ni–Mn/Ni–Co–Mn coatings, the inset shows the comparative total wear volume loss of Ni/Ni–Co and Ni–Mn/Ni–Co–Mn coatings

A similar increase in the size was observed between Ni–47Co and Ni–87Co alloy coatings [12]. Thus, it is seen from the above observations that the introduction of Mn in Ni–Co alloys and plain Co coating resulted in a reduction in the crystallite size due to the change in the diffraction patterns.

3.4 Microhardness

The variation in microhardness of various Ni/Ni–Co alloys and Ni–Mn/Ni–Co–Mn alloy coatings is shown in Fig. 5. The microhardness of Ni, Co and Ni–Co alloy matrices has increased by alloying with Mn. The alloying of Ni with Mn enhanced its microhardness from 250 to 430 HK. The microhardness of Ni–18Co–Mn alloy coating is a maximum of 515 HK. A marginal reduction in microhardness, 490 HK is seen for Ni–47Co–Mn alloy coating. Thus it can be inferred that a Co content of 18 wt% is optimum to produce a hard coating and a further increase in Co content does not enhance the value. This observation is in contrary to that seen for Ni–Co alloy coatings wherein a Co content of 50 wt% is optimum to obtain hard coatings (Fig. 5). Thus, it can be inferred that alloying Ni with 18 wt% Co and small amount (0.40 wt%) of Mn reduces the amount of Co (which is costly) required to obtain a hard coating unlike in the absence of Mn where 40–50 wt% Co content is required [12–14]. Addition of Mn to Ni–87Co alloy exhibited a reduced hardness of 380 HK. This reduction in hardness is due to the change in the crystal structure and the increased crystallite size of the Ni–87Co–Mn alloy. A similar reducing trend is also seen for Ni–87Co alloy (Fig. 5) [12]. The Co–Mn coating is seen to possess an enhanced hardness compared to Ni–87Co–Mn coating and plain Co coating. The increased microhardness can be due to the higher stress associated with the Co–Mn coating.

3.5 Tribological properties

A comparison in the wear volume loss of material for Ni/Ni–Co alloy and Ni–Mn/Ni–Co–Mn alloy coatings is shown in Fig. 6. It is seen from the figure that the alloying of plain Ni, Ni–Co alloys and plain Co with small amount of Mn reduces the volume loss of material resulting in an improved wear resistance. The material loss is remarkable in the case of Mn alloyed plain Ni, Ni–87Co and plain Co coatings. It is also seen from Fig. 6 that the least volume loss in material is exhibited by Ni–18Co–Mn coating or in other words it possesses better wear resistance compared to the other Ni–Mn/Ni–Co–Mn coatings. This improved wear resistance is in accordance with the Archard's law, which states that the hardness is proportional to the wear resistance [19]. The lower wear resistance of Ni–47Co–Mn and Ni–87Co–Mn coatings can be associated with their reduced microhardness. However, the wear resistance of Co–Mn coating is poor compared to Ni–87Co–Mn coating in spite of its higher microhardness. This may be associated with the fact that numerous fine cracks present on the surface of the Co–Mn coating might have resulted in spalling, leading to larger amount of material getting detached from the surface of the Co–Mn alloy coating. Thus it is seen from the above observations that though an enhancement in wear resistance has been observed on the introduction of Mn it is significant only in the case of plain Ni and plain Co coatings.

The wear track of the coatings were analysed to understand the wear behaviour. The wear track profile of various coatings is shown in Fig. 7. Deep wear grooves are observed for Ni–Mn coating while shallow grooves are seen for Ni–18Co–Mn coating. This affirms that the latter has better wear resistance. Deep and broad wear tracks

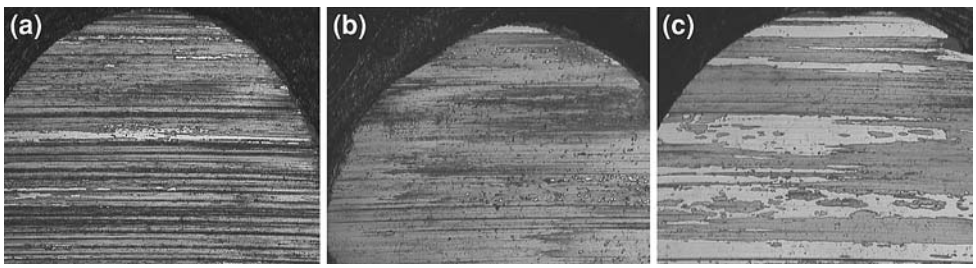

Fig. 7 Wear track profiles of worn pins of **a** Ni–Mn, **b** Ni–18Co–Mn and **c** Co–Mn coatings

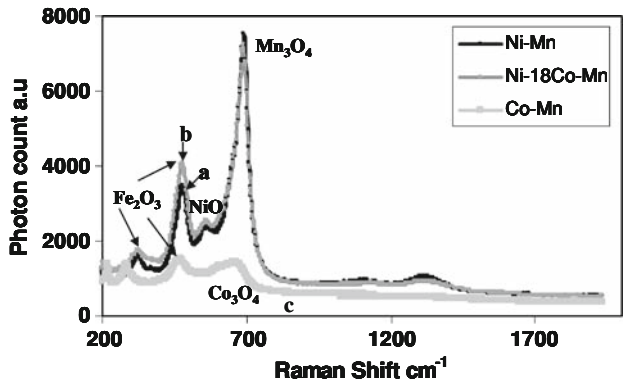

Fig. 8 Raman spectrum of **a** Ni–Mn, **b** Ni–18Co–Mn and **c** Co–Mn alloy coatings wear track on disc

relating to poor wear resistance were observed for Ni–47Co–Mn and Ni–87Co–Mn coatings. However, the worn pin of Co–Mn coating appears as patches of coating with very shallow and narrow wear grooves (Fig. 7c). To further understand this observation, Raman spectra on the wear track of a few representative discs were carried out to identify the nature of the wear debris (Fig. 8). The Raman spectrum of Ni–Mn and Ni–18Co–Mn wear track reveal the presence of Mn_3O_4, NiO, Fe_2O_3 (from the worn disc) [20]. However, the Co–Mn wear track showed less intense oxide peaks of Co_3O_4 and Fe_2O_3. The presence of Mn, Ni and Co oxides can be associated to the fact that during the wear testing a localized rise in temperature occurs resulting in oxide formation. However the presence of iron oxide is due to the contribution from the worn disc. The less intense oxide peaks on Co–Mn wear track can be attributed to the fact that the localized rise in temperature during the wearing away process is less due to the occurrence of spalling, thereby resulting in low oxide formation. The absence of manganese oxide reflection can be related to the presence of very negligible amount of Mn in Co–Mn coating compared to Ni–Mn and Ni–18Co–Mn. The presence of Mn, Ni and Co oxides on the wear tracks of the discs indicates that the transfer of material from the coated pin to the disc has occurred resulting in an adhesive type of wear. Although a difference in the wear performance has been observed, no significant change in the coefficient of friction is seen for all the coatings (0.85–0.90). In other words these coatings can be used for improving wear resistance and not friction reduction.

4 Conclusions

Manganese was incorporated in Ni–Co alloys with different cobalt contents by the process of electrodeposition. Co content was seen to influence the Mn incorporation. The amount of Mn incorporated in various Ni–Co alloys reduced as they became richer in Co content. The alloying of plain Ni, Ni–Co alloys and plain Co coatings with Mn resulted in an improvement in their microhardness and this could be related to the reduction in the crystallite size. A change in crystal structure from fcc to hcp and a change in surface morphology was observed in Ni–Co–Mn alloy with a change in Co content from 47 to 87 wt% similar to that of Ni–Co alloys. Wear testing revealed that Mn introduction substantially improved the wear performance of plain Ni and plain Co coatings. Also, Ni–18Co–Mn exhibited better wear resistance compared to the other Ni–Mn and Ni–Co–Mn coatings. Small cracks present on the surface of Co–Mn coating resulted in its poor wear performance in spite of higher microhardness. Thus it was seen that alloying of Ni with 18 wt% Co and 0.40 wt% Mn produced a coating with enhanced microhardness and wear resistance compared to plain Ni, plain Co and Ni–Co alloy coatings.

Acknowledgements The authors wish to thank Dr. A. R. Upadhya, Director, NAL for permitting to publish the work. The authors are also thankful to Dr. Anjana Jain for the XRD studies and Mr. Raghavendra for the SEM/EDX analysis.

References

1. Marquis EA, Talin AA, Kelly JJ et al (2006) J Appl Electrochem 36:669
2. Dini JW, Johnson HR, West LA (1978) Plat Surf Finish 65:36
3. Wearmouth WR, Bell KC (1979) Plat Surf Finish 66:53
4. Atanassov N, Schils HW (1996) Plat Surf Finish 83:49
5. Ananth MV (1998) Trans Inst Met Finish 76:207
6. Stephen A, Ananth MV, Ravichandran V (1999) Anti-Corros Methods Mater 46:117
7. Atanassov N, Mitreva V (1996) Surf Coat Technol 78:144
8. Yang NYC, Headley TJ, Kelly JJ et al (2004) Scr Mater 51:761
9. Goods SH, Kelly JJ, Yang NYC (2004) Microsyst Technol 10:498
10. Kelly et al. (2004) US 2004/0031691 A1
11. Srivastava M, William Grips VK, Rajam KS (2007) Appl Surf Sci 253:3814
12. Srivastava M, Ezhil Selvi V, William Grips VK et al (2006) Surf Coat Technol 201:3051
13. Safranek WH (1974) The properties of electrodeposited metals and alloys—a handbook. American Elsevier Publishing Co. Inc, New York
14. Dini JW, Johnson HR, Helms JR (1972) Sandia Livermore Laboratories report no. SCL-DR-720090
15. Srivastava M, William Grips VK, Rajam KS (2007) Surf Coat Technol 202:310
16. Malone GA (1987) Plat Surf Finish 74:50
17. Klug HP, Alexander LE (1954) X-ray diffraction procedures. Chapman and Hall, London, chap 9
18. Abd El Rehim SS, Ibrahim MAM, Dankeria MM (2002) Trans IMF 80:105
19. Archard JF (1953) J Appl Phys 24:981
20. Liang C-H, Hwang C-S (2008) Jpn J Appl Phys 47:4682